



OPEN EEG-based functional and effective connectivity patterns during emotional episodes using graph theoretical analysis

Majid Roshanaei¹, Hamzeh Norouzi¹, Julie Onton², Scott Makeig² & Alireza Mohammadi³✉

Understanding the neural mechanisms underlying emotional processing is critical for advancing neuroscience and mental health interventions. This study examined these mechanisms by analyzing EEG connectivity patterns across different brain regions while participants evoked various emotions. After applying independent component analysis (ICA) to eliminate non-cortical activity, we assessed frequency-specific connectivity patterns using coherence, Granger causality, and graph theoretical measures to evaluate both functional and effective connectivity. Graph theoretical analysis revealed significant differences in connectivity between emotions across multiple frequency bands, particularly in the delta and beta bands. These results indicated modulations in key brain regions, such as the precentral, superior frontal, and temporal areas, suggesting that these regions play a crucial role in emotional processing. Coherence analysis demonstrated predominant alpha band activity across all emotions, with specific emotional states, such as fear, grief, and jealousy, exhibiting enhanced beta band activity. In terms of coherence strength, we observed that the gamma band was largely inactive, except for the emotion of sadness, which displayed significant activity in the right lobe, particularly in regions such as the supplementary motor area and the lingual gyrus. Additionally, Granger causality analysis highlighted that the beta and gamma bands were dominant across all emotional states, with minimal modulation observed in the theta band. Clustering coefficients from the graph analysis further revealed distinct patterns of connectivity in the delta and beta bands, with significant variations across different emotions, particularly in the temporal and frontal regions. These findings enhance our understanding of emotional processing and have practical applications in mental health, biomarker identification, and human-computer interaction.

Keywords EEG connectivity, Emotional states, Coherence analysis, Granger causality, Graph theoretical analysis, Brain networks

Emotion regulation plays a central role in human cognition, behavior, and social interactions, shaping our experiences and influencing decision-making processes^{1,2}. Understanding the neural mechanisms underlying emotions has long been a focus of neuroscience, with advancements in neuroimaging providing insights into the relationship between brain activity and emotional states^{3–5}. Among these techniques, electroencephalography (EEG) stands out due to its high temporal resolution and non-invasiveness, making it a valuable tool for studying real-time brain dynamics during emotional processing^{6–8}.

James Gross's work on emotion regulation strategies provides a framework for understanding how individuals modulate their emotional responses through reappraisal and suppression⁹. These strategies include cognitive reappraisal, in which individuals reinterpret emotional stimuli, and expressive suppression, where emotional expressions are inhibited. The adaptive nature of emotion regulation promotes psychological well-being and enhances social functioning¹⁰.

Recent advancements in EEG-based functional and effective connectivity patterns have improved the interpretation of emotional states^{11,12}. Understanding emotions increasingly depends on connectivity metrics that quantify the interdependencies among brain regions¹³. Techniques such as Granger causality, coherence,

¹Student Research Committee, Baqiyatallah University of Medical Sciences, Tehran, Iran. ²Swartz Center for Computational Neuroscience, University of California San Diego, 9500 Gilman Drive, La Jolla, CA 92093, USA. ³Neuroscience Research Center, Baqiyatallah University of Medical Sciences, Tehran, Iran. ✉email: ar.mohammadi@bmsu.ac.ir

and graph theory analysis have proven instrumental in unraveling the complex networks that underlie emotional experiences¹⁴.

Coherence analysis has revealed frequency-specific synchronization patterns in EEG that characterize emotional states. Enhanced theta (4–7 Hz) and alpha (8–12 Hz) coherence are linked to relaxation and positive emotions, particularly in the frontal and parietal regions^{15,16}. Increased beta (13–30 Hz) coherence is associated with anxiety and involves the prefrontal cortex¹⁷. Heightened gamma (30–100 Hz) coherence in the prefrontal and temporal lobes corresponds to intense emotions such as fear and excitement¹⁸, while decreased delta (1–4 Hz) coherence in the anterior cingulate cortex is associated with emotional dysregulation and depression¹⁹. These results illustrate the complex synchronization patterns in the brain during various emotional states, highlighting the significance of specific frequency bands and brain regions.

Moreover, Granger causality analysis has elucidated directional interactions between brain regions during emotional processing^{20,21}. For instance, it is demonstrated that the directional influence from the amygdala to the prefrontal cortex is significant during fear processing, particularly in the beta and gamma frequency bands²⁰. Also, it is shown that during emotional memory recall, there are prominent directional interactions from the hippocampus to the prefrontal cortex, especially in the theta band²¹. Additionally, the directional beta band connectivity from the occipital to the frontal regions is raised when viewing emotionally salient images, indicating a feedforward process of emotional information²². Furthermore, another study highlighted that gamma band Granger causality from the anterior cingulate cortex to the amygdala is associated with regulating negative emotions²³. These findings reveal the intricate directional interactions between brain regions and specific frequency bands that are involved in the dynamic processing of emotional states.

Recent studies have demonstrated the value of graph theoretical approaches in analyzing EEG data to uncover neural connectivity patterns associated with various emotional states. For instance, a study by Aydın et al.²⁴ utilized graph theoretical measures to investigate the neural correlates of emotions such as fear and anger, which were induced by specific musical rhythms. Their research highlighted how different emotional states modulate brain connectivity patterns, particularly in regions such as the amygdala and prefrontal cortex, and how these patterns vary with emotional intensity²⁴. Additionally, a study by Kılıç et al.²⁵ focused on classifying contrasting discrete emotional states using EEG-based graph theoretical network measures. By examining the connectivity structure of the brain during different emotional states, including happiness, sadness, and anger, they developed a model capable of differentiating these emotions based on distinct brain network signatures, such as changes in coherence and network modularity²⁵. Graph theoretical approaches have furthered our understanding of the brain's network architecture during emotional experiences. By mapping EEG connectivity onto graph representations, researchers have identified key network properties associated with different emotional states²⁶. Notably, some research has highlighted the role of network modularity and efficiency in shaping emotional processing dynamics^{27,28}. There is also increased beta-band activity during experiencing anxiety, particularly in the prefrontal cortex and amygdala, indicating increased alertness and emotional arousal²⁹. In contrast, relaxation and positive emotions are connected to enhanced alpha-band coherence, involving regions such as the posterior cingulate cortex and parietal lobes, reflecting a state of calm and internal focus³⁰. Additionally, theta-band activity has been linked to emotional memory processing, engaging the hippocampus and frontal regions²⁶. These findings emphasize the complexity of brain network interactions across various emotional states, offering insights into how specific brain regions and frequency bands contribute to our emotional experiences. Building on these insights, our study employs graph theoretical measures to explore EEG connectivity patterns across multiple emotional states, utilizing a dimensional model of emotion. This model captures the continuous spectrum of emotional experiences, enabling us to analyze both positive and negative emotional states. Through this approach, we aim to provide a more nuanced understanding of how specific brain networks, including the frontal, temporal, and parietal regions, are activated during a range of emotional experiences.

The work of Onton and Makeig has significantly expanded our understanding of brain activity during emotional experiences through Independent Component Analysis (ICA) of EEG data³¹. They identified that emotional stimuli evoke specific patterns of brain activity in different frequency bands. Their research shows that the prefrontal cortex is notably active in the beta and gamma bands during emotional processing, indicating its role in cognitive and emotional regulation³¹. Furthering their investigation, they revealed that positive emotions, such as happiness and contentment, are associated with increased alpha and theta band activity in the parietal and occipital lobes³². These areas are linked to sensory integration and memory processes, respectively. The anterior cingulate cortex (ACC), dorsolateral prefrontal cortex (DLPFC), and amygdala have been demonstrated to be the primary brain regions involved in emotion regulation and processing³³.

Regarding frequency bands, the theta and alpha bands exhibited significant modulations during the emotion imagination task, reflecting changes in cognitive and emotional states³⁴. They also investigated emotion recognition from EEG during self-paced emotional imagery and identified the key brain areas and frequency bands involved in emotional processing³⁵. The frontal regions, including the prefrontal cortex and anterior cingulate cortex, were found to exhibit distinct patterns of connectivity during emotional imagery tasks. Specifically, the theta and beta frequency bands showed significant modulations, indicating cognitive and affective processing associated with emotion recognition. Their comprehensive analysis underscores the intricate frequency-band-specific and region-specific dynamics involved in emotional experiences³⁵.

Despite these developments, research on the connectivity patterns between various subtle emotional states is still lacking. Onton and Makeig's studies focus primarily on broad emotional categories and the activity within individual brain regions or networks^{32,34}. Less is known, though, about the precise connections and interactions that occur between these areas during various emotional experiences. This gap is crucial because emotions depend on context and are complicated, necessitating a deeper examination of the patterns of connectivity that distinguish between them. Our research seeks to close this gap by applying innovative EEG analysis techniques to examine the connections among various emotional states. We aim to provide a more thorough understanding of

the brain's emotional processing by looking at the specific neural interactions and their frequency characteristics. This could have important implications for affective neuroscience and mental health interventions.

In this context, our study aims to contribute to the ongoing dialogue on emotional connectivity by conducting an in-depth analysis of EEG datasets in various emotional states. By employing a comprehensive methodology that integrates coherence, Granger causality, and graph theoretical analysis, we seek to unravel the complex neural signatures underlying emotions and their implications for cognitive and affective neuroscience. In particular, our methodology entails meticulous preprocessing steps like eliminating non-brain activity via ICA decomposition to ensure the quality and reliability of EEG signals, followed by the application of coherence analysis to identify frequency-specific connectivity patterns. Granger causality analysis is then utilized to uncover directional influences between brain regions, providing insights into the causal relationships that characterize emotional processing. Graph theoretical analysis further enhances our understanding by revealing the topological properties of brain networks, such as modularity, clustering coefficients, and degree centrality, across different emotional states.

Our research aims not only to advance scientific understanding of emotional processing, but also to pave the way for innovative applications that leverage EEG-based insights to improve human-computer interactions, mental health diagnoses, and personalized therapies. Our findings possess the capacity to influence the development of affective computing systems that can more accurately detect and respond to human emotions, thereby improving user experiences in various technological interfaces. Additionally, by elucidating the neural basis of emotional states, our work may contribute to the development of targeted mental health interventions and personalized therapeutic strategies to address conditions such as depression, anxiety, and mood disorders. Ultimately, this study hopes to bridge the gap between basic neuroscience research and practical applications and promote a deeper integration of EEG-based emotional insights into real-world contexts.

Materials and methods

Dataset

This study used a dataset of 250 scalp channels EEG recordings from 34 volunteers that were obtained and prepared according to the explanations of Onton and Makeig³⁶. You can access the data (obtained at Prof. Scott Makeig's Lab) directly on the NEMAR website (https://nemar.org/dataexplorer/detail?dataset_id=ds003004; look for Imagined Emotion Study). A Biosemi ActiveTwo system (Amsterdam, Netherlands) recorded EEG data from 250 channels on the scalp at 256 Hz per channel and 24-bit resolution. The electrodes were placed on most of the scalp, forehead, and lateral face surface using caps with a custom whole-head montage, but not on the chin and fleshy cheek areas. The 3D locations of the electrodes relative to each participant were also measured (Polhemus, Inc.). For more information, refer to Onton and Makeig²⁹ and the NEMAR website description. All methods were conducted in accordance with the relevant guidelines and regulations outlined in the study protocol approved by the Research Ethics Committee of Baqiyatallah University of Medical Sciences (approval code: IR.BMSU.REC.1402.049).

Experiment and participants

The emotion imagination experiment involved 34 volunteers who gave informed consent according to the UCSD institutional review board standards. The participants said they could create realistic emotional feelings for most of the emotions they were asked to imagine by listening to a recorded voice guide and using their imagination. For instance, for anger, the voice guide asked them to remember or imagine a situation that would make them angry and gave two examples (Someone is hitting your car with a baseball bat for no reason). The participants sat comfortably with their closed eyes in a dim, and quiet room and heard the voice guides through earbud headphones.

The paradigm of the self-paced emotional imagery experiment is shown in Fig. 2A. Each session began with 2 min of quiet eyes-closed rest, followed by recorded general instructions, and then a 5 min relaxation induction to help the participant achieve a calm, inward-focused state of mind. Next, participants listened to a series of recorded voice-guided inductions that asked them to remember or imagine situations that would evoke a strong, embodied feeling of the emotion they were told to imagine. Participants were advised to focus on their physical state as this would make their emotional experience more intense and lasting³⁴. Participants could take as long as they wanted to remember or imagine a situation, that would give them feel the emotion they were supposed to imagine. There were no external time constraints or cues. Participants pressed a thumb button on their right hand once they started to feel the emotion they were aiming for, then a thumb button on their left hand when the imagined situation and feeling started to fade, which triggered (40 s) instructions to relax again (followed by a silent 10 s period), letting go of the scene and feeling they had just experienced. Then 10-second audio clip prepared them for the next emotion imagination period.

The participants listened to a series of 15 emotional imagination periods in the same pseudo-random order that switched between one of eight positive emotions (love, joy, happiness, relief, compassion, contentedness, excitement, awe) and one of seven negative emotions (anger, jealousy, disgust, frustration, fear, sadness, grief). The whole experiment took about 80 min. The participant pressed a button to mark the start and end of each emotion imagination period, which ranged from 43 s to 12 min, with most being 3 to 5 min long. The voice prompts that evoked the emotions can be found in the Onton and Makeig supporting information²⁹.

Data preprocessing

The data were preprocessed according to the protocols established by Onton and Makeig²⁹. Initially, defective channels—such as electrodes with poor skin contact, identified by their abnormal activity patterns—were removed, resulting in a range of 134 to 235 channels per subject (214 ± 18 ; mean \pm SD)³². Data segments exhibiting high-amplitude muscle noise and other irregular artifacts, identified through high-kurtosis or low-

probability tests, were excluded using EEGLAB functions^{37,38}. The data were subsequently downsampled to 100 Hz, ensuring the preservation of information below 50 Hz to minimize interference from line noise, as the line noise frequency in the dataset is 60 Hz³⁹. Preprocessing adhered to Makoto's preprocessing pipeline (https://sccn.ucsd.edu/wiki/Makoto%27s_preprocessing_pipeline), which included re-referencing to average channels and applying a digital filter to retain frequencies above 0.1 Hz³⁹. The remaining data were concatenated and subjected to full-rank decomposition via extended infomax ICA using the *binica* function⁴⁰ in EEGLAB (<http://sccn.ucsd.edu/eeqlab>). Independent components (ICs) from each subject were evaluated using the ICLabel plugin in EEGLAB⁴¹ to identify brain-related components. A component was classified as brain-related if it had a probability score exceeding 90%. Non-brain artifacts, such as muscle activity, line noise, or eye movements, were excluded. The scalp map of brain-related ICs for a single subject is depicted in Fig. 1A. After removing non-brain artifacts, 13 ICs remained for the sample subject, with the number of ICs ranging from 6 to 32 across subjects (16.9 ± 6.221 ; mean \pm SD). These ICs represent contributions from various brain lobes, including the frontal, occipital, temporal, and parietal regions. Source localization was subsequently performed using the *ft_sourceanalysis* function in the FieldTrip toolbox⁴² mapping the resulting sources to 32 regions of interest^{43,44}. Table 1 presents the full names and abbreviations of 32 brain regions^{43,44}. Additionally, a lateral view of these brain regions is shown in Fig. 1B, which was generated using the BrainNet Viewer MATLAB toolbox (<http://www.nitrc.org/projects/bnv/>)⁴⁵. All methods were conducted in accordance with the relevant guidelines and regulations outlined in the study protocol approved by the Research Ethics Committee of Baqiyatallah University of Medical Sciences (approval code: IR.BMSU.REC.1402.049).

Connectivity measures

EEG data were analyzed using functional and effective connectivity methodologies, including coherence and Granger causality, as well as criteria derived from graph theory. In our study, we integrated coherence and Granger causality to capture both spectral and causal aspects of connectivity. The frequency bands were defined as follows: 1–5 Hz for delta, 5–8 Hz for theta, 8–14 Hz for alpha, 15–30 Hz for beta, and 30–49 Hz for gamma. Coherence provides insights into the synchronization of brain regions in the frequency domain, while Granger causality offers temporal directionality, identifying causal relationships between regions. By employing both methods, we aimed to create a more comprehensive understanding of the interactions between brain regions across both frequency and time domains. This combination of methodologies enabled us to assess various facets of connectivity and interactions that may not be fully captured by either method alone. Below is a brief explanation of the theoretical foundations underlying each approach.

Coherence

In our EEG data analysis, we employed coherence as a connectivity measure to unravel the synchronized neural activity between different brain regions⁴⁶. Coherence quantifies the degree of linear coupling between two signals in various frequency bands, providing insights into the functional connectivity underlying cognitive processes. Mathematically, coherence between two signals X and Y at a frequency (f), denoted as $C_{XY}(f)$, is computed as the magnitude squared coherence, given by:

$$C_{XY}(f) = \frac{|P_{XY}(f)|^2}{P_{XX}(f) \cdot P_{YY}(f)} \quad (1)$$

Where $P_{XY}(f)$ is the cross-spectral density between X and Y , and $P_{XX}(f)$ and $P_{YY}(f)$ are the respective power spectral densities, calculated as the absolute value of the Fourier spectrum using the MATLAB Toolbox-FieldTrip (<https://www.fieldtriptoolbox.org>)⁴². Coherence ranges from 0 to 1, with higher values indicating stronger coupling. Its application in EEG data analysis enables us to discern frequency-specific connectivity patterns, illuminating the coordinated neural processes during cognitive tasks.

Granger causality

In our investigation of EEG data connectivity, we leveraged Granger causality³⁶, a robust time-series analysis method that facilitates the quantification of directional interactions between different brain regions. Granger causality is grounded in the notion that if the past values of one time series enhance the prediction of another, then the former is said to “Granger cause” the latter. Mathematically, for a two-time series X and Y , the Granger causality from X to Y (denoted as $GC_{X \rightarrow Y}$) can be expressed as a reduction in the forecast error Y when incorporating past values of X . This is formalized by the following equation:

$$F_Y(t) = \sum_{i=1}^p a_i Y(t-i) + \sum_{j=1}^p b_j X(t-j) + \epsilon(t) \quad (2)$$

Where $F_Y(t)$ represents the forecast of Y at time t based on its past values and the past values of X , a_i , and b_j are coefficients, p is the model order, and $\epsilon(t)$ is the prediction error. The $GC_{X \rightarrow Y}$ is subsequently determined by evaluating the statistical significance of the coefficients b_j . This analytical framework enables us to discern the effective connectivity patterns within the brain, providing valuable insights into the information flow dynamics during cognitive processes. Before conducting the Granger causality analysis, the SIFT toolbox in EEGLAB was utilized to determine the autoregressive (AR) model order. The AR model order was set within a range of 1 to 50, and the Vieira-Morf algorithm, in conjunction with the Akaike Information Criterion (AIC), was employed to adaptively select the optimal model order for each subject, thereby ensuring minimal error. Additionally, we conducted a sanity check on the fitted AR models for each subject by examining the whiteness

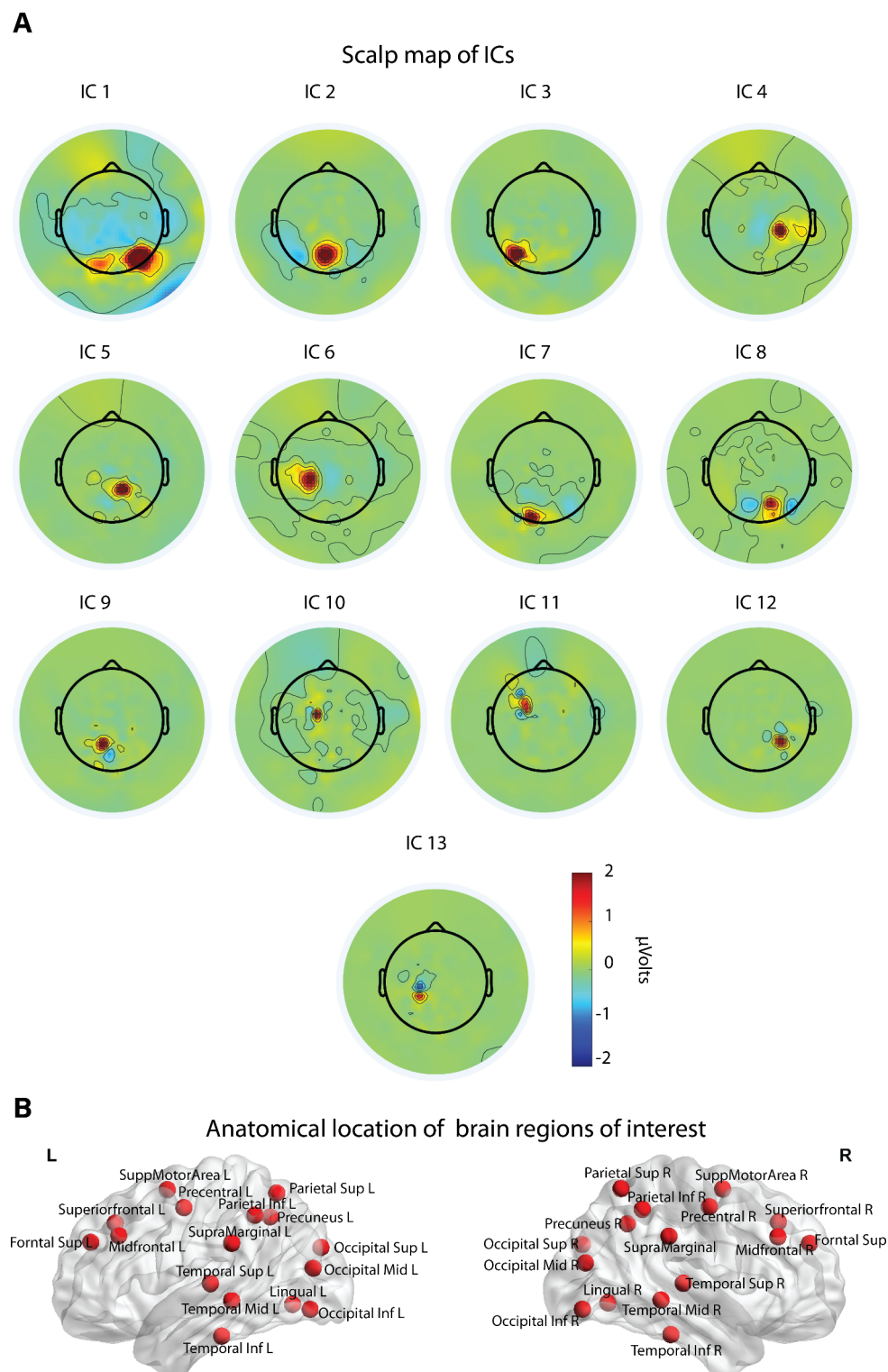


Fig. 1. Scalp map of brain-related independent components (ICs) and the anatomical locations of brain regions of interest, generated using the BrainNet Viewer MATLAB toolbox. **(A)** Scalp map of brain-related ICs for a single subject. After removing non-brain artifacts, 13 ICs remained, with contributions from various brain lobes, including the frontal, occipital, temporal, and parietal regions. **(B)** Anatomical locations of brain regions of interest are shown from the left and right lateral views of the brain.

No.	Brain region	Abbreviation	No.	Brain region	Abbreviation
1	Left precentral	Precentral_L	17	Left inferior occipital	Occipital_Inf_L
2	Right precentral	Precentral_R	18	Right inferior occipital	Occipital_Inf_R
3	Left Superior Frontal	Superiorfrontal_L	19	Left superior parietal	Parietal_Sup_L
4	Right Superior Frontal	Superiorfrontal_R	20	Right superior parietal	Parietal_Sup_R
5	Left middle frontal	Midfrontal_L	21	Left inferior parietal	Parietal_Inf_L
6	Right middle frontal	Midfrontal_R	22	Right inferior parietal	Parietal_Inf_R
7	Left supplementary motor area	SuppMotorArea_L	23	Left supramarginal	SupraMarginal_L
8	Right supplementary motor area	SuppMotorArea_R	24	Right supramarginal	SupraMarginal_R
9	Left Superior Medial Frontal	Frontal_Sup_Medial_L	25	Left precuneus	Precuneus_L
10	Right Superior Medial Frontal	Frontal_Sup_Medial_R	26	Right precuneus	Precuneus_R
11	Left lingual	Lingual_L	27	Left superior temporal	Temporal_Sup_L
12	Right lingual	Lingual_R	28	Right superior temporal	Temporal_Sup_R
13	Left superior occipital	Occipital_Sup_L	29	Left middle temporal	Temporal_Mid_L
14	Right superior occipital	Occipital_Sup_R	30	Right middle temporal	Temporal_Mid_R
15	Left middle occipital	Occipital_Mid_L	31	Left inferior temporal	Temporal_Inf_L
16	Right middle occipital	Occipital_Mid_R	32	Right inferior temporal	Temporal_Inf_R

Table 1. Information on brain regions.

of the residuals. This process involved ensuring that the residuals—the differences between the observed and predicted values—were randomly distributed and exhibited no discernible patterns, indicating “white noise”. This step was essential for verifying the reliability of the AR models before proceeding with the analysis.

Graph analysis

We derived coherence and Granger causality measures from 160-second EEG epochs for each emotion within a single trial. Band-specific adjacency matrices were frequently generated for each connectivity measure, serving as weighted adjacency matrices. These matrices were then subjected to graph-theoretical analysis^{28,47}. In this framework, the brain is conceptualized as a graph whose nodes represent brain regions or ICA component activations and whose edges embody functional and effective connectivity as determined by coherence and Granger causality. Connectivity measures were computed using algorithms from the MATLAB Toolbox-FieldTrip (<https://www.fieldtriptoolbox.org>)⁴², while graph-theoretical indices were derived using functions from the Brain Connectivity Toolbox (<http://www.brain-connectivity-toolbox.net>).

Graphs obtained from the connectivity measures were analyzed for various indices: (1) basic measures such as density, degree, and strength, and (2) segregation measures like the clustering coefficient^{25,37,48}. Additionally, transitivity and modularity were calculated. The degree of a node, which indicates its centrality, corresponds to the number of its connections and reflects the number of its adjacent nodes. The mean degree of the network serves as an indicator of the graph density or the total connectivity cost of the network. In directed graphs, the degree differentiates between incoming and outgoing connections, while strength, a weighted variant, sums the weights of all neighboring connections⁴⁷.

Segregation measures, such as the clustering coefficient, quantify the network’s capacity for specialized processing within highly interconnected clusters of nodes. The clustering coefficient measures the extent to which a node’s neighbors are connected and reflects local node cohesion⁴⁹.

Modularity and transitivity are central concepts in network science and provide insights into the structural organization of complex networks^{41,42}. Modularity is a measure that quantifies the strength of dividing a network into different modules or communities. A network with high modularity has dense connections within its modules and sparse connections between them, suggesting a strong community structure⁴¹. On the other hand, transitivity, also known as the global clustering coefficient, is the ratio of the number of triangles to the number of triplets in the network. It reflects the degree to which nodes in a network tend to band together and form tightly-knit groups⁴². High transitivity indicates that neighboring nodes are likely to be connected, indicating the presence of coherent subgroups within the network. Modularity and transitivity provide a comprehensive view of the network’s tendency toward compartmentalization and coherent grouping, which are essential for understanding the dynamics and functionality of various systems, from social interactions to biological networks.

Statistical analysis

In the created adjacency matrix, connectivity values that exceeded a significance threshold were retained ($p < 0.05$), while values below this threshold were reset to zero. The statistical significance of these connectivity values was determined by surrogate data analysis⁴³, a method that preserves the amplitude of the original signals but disrupts their phase relationships. This is achieved by randomizing the data within the frequency domain before converting it back to the time domain. To assess significance, the connectivity values of the original data were compared with those derived from the surrogate data (see also [Supplementary Information](#)). A total of 200 surrogate instances were generated for each signal to perform this comparison⁵⁰.

A Wilcoxon signed-rank test was utilized to identify distinct connectivity patterns between the two groups (i.e., emotions and pre-baseline activity), and a Wilcoxon signed-rank test was applied to the graph indices. To

account for multiple comparisons, we applied the false discovery rate (FDR) correction to the resulting p -values. Significant elements were identified based on an adjusted threshold of $p < 0.05$, indicating connectivity changes associated with the emotional task relative to the pre-baseline (see also Supplementary Table S1).

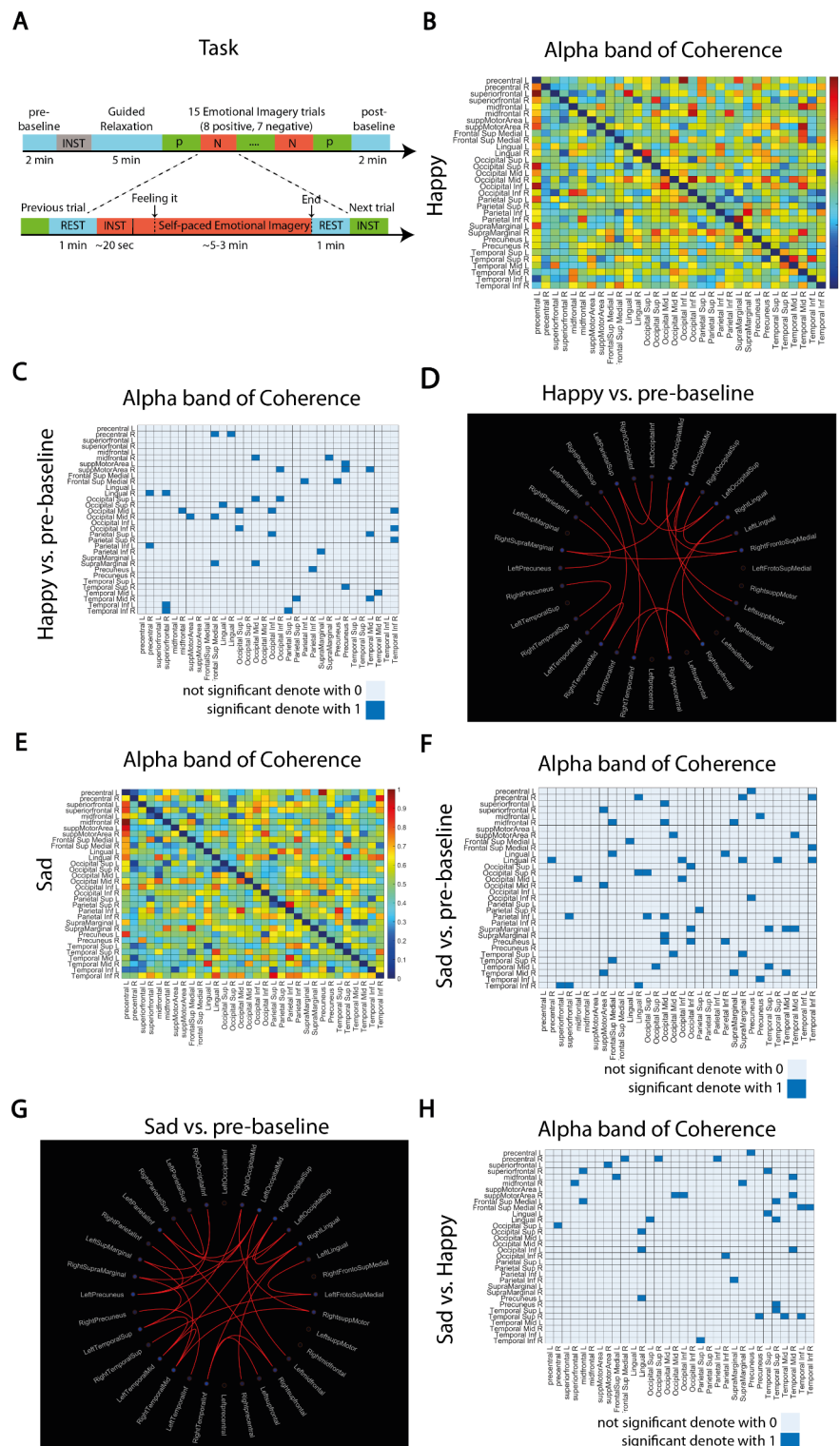
Results

ICA component activations were documented in various brain regions to investigate the impact of different emotions on brain electrical activity. At the same time, the subjects tried to evoke certain feelings, as described in the previous section. Figure 2 shows the coherence connectivity results for two contrasting emotions within the alpha frequency band. Figure 2B shows the normalized coherence for a happiness state and displays which brain regions exhibit significant deviations from baseline activity. This was determined by comparing the happy state to the pre-baseline period, with the results depicted in Fig. 2C,D. Connectivity patterns that show significant differences from the pre-baseline are indicated by a value of 1, as determined using the Wilcoxon signed-rank test (described in the Statistical Analysis section). Conversely, connectivity patterns that show no deviations are categorized as zero ($p < 0.05$, Wilcoxon test). To illustrate, the precentral_R area displayed connectivity with the Frontal_Sup_Medial and Lingual regions and showed activity in the occipital and temporal areas. Figure 2E presents the normalized coherence for a state of sadness. To identify brain regions demonstrating significant deviations from their baseline activity, we assessed the sad state in comparison to the pre-baseline period (Fig. 2F,G). Connectivity patterns that exhibit noteworthy differences compared to the pre-baseline condition are marked with a value of 1, while those that do not exhibit any differences are indicated as zero ($p < 0.05$, Wilcoxon test). In this emotional state, the results reveal predominantly activity in the frontal and temporal areas. To facilitate a comparison between these two contrasting emotions, Fig. 2H displays the significance test of the coherence results in the alpha band for both happy and sad states. The frontal and temporal areas show notable modulations, including the superiorfrontal, Frontal_Sup_Medial, Temporal_Sup, and Mid regions.

Figure 3 presents a statistical comparison utilizing the Wilcoxon signed-rank test (as described in the statistical analysis section) to assess the coherence connectivity between eight positive and seven negative emotions related to pre-baseline activity. This comparison is carried out for five frequency bands for each brain region. The subplots within the figure consist of 32×32 adjacency matrices, each depicting the significance of activity in the brain regions. A value of “1” indicates significant activity for a specific emotion compared to pre-baseline activity within a frequency band, while a value of “0” indicates no significant activity. The rows of the matrices represent different emotions, and the columns correspond to the results for each frequency band. Notably, alpha-band activity is the predominant activity in all emotions, with significant beta-band activity observed in three negative emotions: fear, grief, and jealousy. Compared to other emotions in this frequency range, increased gamma band activity is observed in states of excitement, frustration, jealousy, and sadness. For most emotions, alpha-band activity is predominantly present in the frontal and temporal areas. For example, during anger, significant alpha-band activity is detected in the precentral_L and Occipital_Sup_R channels, as well as in the Temporal_Mid_L&R regions. In the case of awe, there is not only activity in the frontal and temporal areas but also a discernible connection between the parietal and temporal regions. For the emotion of jealousy, pronounced connectivity is illustrated between the frontal and linguistic areas. The figure allows for the extraction of all such connections for each emotion in the various frequency bands.

Figure 4 parallels the results of Fig. 3 but focuses on Granger causality connectivity measures. The rows of each matrix represent information “from” a brain region, while the columns represent information “to” a brain region. For instance, during the experience of anger in the beta band, there is a Granger causality connection from brain region 2 to brain region 8, whereas the reverse direction is not observed. Here, the beta and more powerful gamma bands were identified as the dominant frequency bands in all emotions, with minimal to no modulation observed in the theta band. Among different emotions, sadness, anger, awe, happiness, and frustration exhibited greater activity in the gamma band compared to other emotions. Additionally, sadness and frustration showed increased coherence connectivity in the gamma band, as previously mentioned. In the gamma band, a robust causal connection is evident between the Occipital_Sup_L region and most areas for emotions such as anger, awe, compassion, excitement, fear, frustration, grief, happiness, love, relief, and sadness. The same gamma-band activity is apparent between the Occipital_Sup_L channel and the parietal region for emotions of disgust, contentment, and joy. Moreover, a strong gamma-band causal connection is present between the middle temporal region and all other areas for the majority of emotions. A similar pattern of connectivity is observed in the beta band. In contrast, a weak delta band activity is depicted in the temporal region in most emotions. To enhance clarity and minimize confusion arising from the variety of emotions, frequency bands, and brain regions, we focused on graph analysis to more effectively illustrate connectivity patterns. In Figs. 3 and 4, brain regions are labeled numerically to simplify the identification of specific regions and improve the clarity of the presented data. This approach enables a more straightforward interpretation of the results, reducing the complexity of labeling the figures while still conveying essential information. In Figs. 2 and 3, the brain region labels are represented numerically from 1 to 32 to enhance clarity.

In the analysis presented in Fig. 5, we identified statistically significant differences in the level of connectivity between different emotions and pre-baseline activities within each of the 32 selectively selected brain regions. These variations were consistent in all frequency bands and connectivity metrics evaluated. Notably, within the beta band coherence connectivity metric, most emotions exhibited modulations primarily in the Lingual_R area and occipital lobe, such as Occipital_Sup_L&R, Occipital_Mid_R, and Occipital_Inf_R area. Furthermore, emotions such as awe, contentment, disgust, excitement, grief, love, and joy demonstrated modulations in the frontal region, albeit to a lesser extent. In other frequency bands, emotion-related modulations were observed in the frontal, occipital, and parietal lobes. For instance, in the context of the theta frequency band, various emotions such as fear, frustration, joy, relief, and sadness were associated with significant alterations in the



level of coherence measure in the Parietal_Sup_L&R areas. Within this frequency band, minimal activity was observed in the frontal and temporal regions.

The second column of Fig. 5 delineates the results of the degree measure for Granger causality connectivity with more dominance in delta and beta bands. In the delta band, a majority of emotions corresponded with modulatory activity in the precentral and superior frontal regions, alongside the parietal and temporal areas like Parietal_Inf_L, SupraMarginal_L&R, Temporal_Sup_R, and Temporal_Inf_R areas. Additionally, the beta band revealed pronounced modulations, with most emotions inducing modulation in connectivity in the precentral, lingual, parietal, and temporal regions such as precentral_R, suppMotorArea_L, Lingual_L&R, Parietal_Sup_L, Temporal_Sup, and Temporal_Inf areas. Across the remaining frequency bands, discernible modulations in the frontal, occipital, and temporal regions were associated with specific emotions, though not as prominently as in the delta and beta bands (See additional information in Fig. 5).

◀ **Fig. 2.** Task and Connectivity Analysis for Contrasting Emotions. **(A)** Experimental paradigm for the self-paced emotion imagination task. Each session consisted of a pre-baseline period, followed by a guided relaxation phase. This was followed by 15 emotion imagination trials alternating between positive and negative emotions, with a post-baseline period at the end. **(B)** Normalized coherence connectivity in the alpha band for a happy emotional state in 32 brain regions, Coherence ranged from 0, indicating no coherence, to 1, indicating full coherence. **(C)** Statistical comparison of alpha band coherence between happiness and pre-baseline at various brain regions, with significant changes indicated by 1 and non-significant changes indicated by 0. **(D)** Connectivity map between brain regions, highlighting significant differences in coherence during the happy state compared to the pre-baseline. **(E)** Normalized coherence connectivity in the alpha band for a sad emotional state in 32 brain regions, Coherence ranged from 0, indicating no coherence, to 1, indicating full coherence. **(F)** Statistical comparison of alpha band coherence for happiness versus pre-baseline at various brain regions, with significant changes indicated by 1 and non-significant changes indicated by 0. **(G)** Connectivity map between brain regions, highlighting significant differences in happy state coherence compared to pre-baseline, **(H)** Comparative statistical analysis of alpha-band coherence between happy and sad emotional states at different sites, with significant changes indicated by 1 and non-significant changes indicated by 0.

Figure 6 shows a statistically significant deviation in connectivity strength between different emotions and pre-baseline activities. The first column, focusing on coherence connectivity, indicates that within the delta band, emotions such as contentment, disgust, excitement, fear, jealousy, relief, and sadness are linked to activity in the frontal, occipital, and parietal regions such as the midfrontal_L, Occipital_Inf_L, Parietal_Sup_R, and Temporal_Sup_R area. The theta, alpha, and beta bands display intermittent activity corresponding to different emotions, while the gamma band is predominantly inactive, except for the emotion sadness, which is mainly active in the right lobe of the brain such as supMotorArea_R, Lingual_R, Occipital_Mid_R, Parietal_Inf_R, supraMarginal_R, and Temporal_Inf_R areas. The second column, which presents the results of the Granger causality measurement, shows that the delta and beta bands are the most dynamically active frequency bands. It is noteworthy that in the delta band the regions superiorfrontal_L, Parietal_Inf, supraMarginal, and temporal_Sup_R show the greatest activity for the majority of emotions. In the beta band, significant activity is observed in all temporal regions for nearly all emotional states, with additional activity in the precentral_R, supMotorArea, and Parietal_Sup_L regions. The theta, alpha, and gamma bands show sporadic activity in various brain regions. For instance, in the alpha band, emotions such as frustration, grief, and compassion are associated with modulations in the linguistic area. In the gamma band, emotions of happiness and relief are active across most of the parietal area, for more details about the activity of each region in each frequency band for each emotion can be found in Fig. 6.

Figure 7 presents the connectivity modularity results, which are consistent with the results from Figs. 5 and 6. In the area of coherence connectivity, delta and alpha bands are the most active frequency bands, the alpha band exhibits distinct modulations for certain emotions in the supramarginal region. Furthermore, negative emotions such as disgust, fear, and grief demonstrate activity in the Lingual and Frontal_Sup_Medial areas. A similar pattern of activity is observed in the delta, beta, and gamma bands, with significant activity in the supplementary motor and temporal regions. Theta frequency bands show capricious activity in different brain regions. In terms of the Granger causality measure, the delta and beta bands are the most active frequency bands, as the degree and strength measures are the same. The delta band predominantly displays activity in the frontal and parietal areas such as midfrontal, Parietal_Sup, and Inf areas with occasional activity in the occipital and temporal regions. Theta band activity is notable in the lingual and parietal areas. The alpha band primarily reveals activity in the frontal region. Importantly, the most active regions of the beta band include the frontal lobe, particularly the precentral and superior frontal areas, as well as the occipital Inf and parietal regions, which include the supramarginal and precuneus areas, with the gamma band showing intermittent activity, including the Occipital_Inf and Mid areas and Temporal_Mid regions.

Figure 8 illustrates statistically significant differences between numerous emotions and pre-baseline activity in frequency bands in graph connectivity measures. The first column presents the results for clustering coefficients. Notably, the coherence measure in the alpha band is significantly different for content emotion, while in the delta band, emotions such as content, fear, jealousy, and relief show statistical differences from pre-baseline activity. When considering the Granger causality metric, the clustering coefficient indicates greater variations within the delta and beta frequency ranges, aligning with findings from prior graph analyses. The clustering coefficient demonstrates variations in most emotional responses within the delta and beta frequency bands, as well as in certain emotional states within the alpha and gamma bands, compared to pre-baseline activity levels. Regarding the density metric, both coherence and Granger causality unveil notable distinctions in specific emotional states in various frequency bands. For example, in coherence, awe is active in the beta band, contentment is active in the delta band, and joy and relief are active in the theta band. Lastly, the transitivity measure for coherence connectivity demonstrates significance for three emotions compared to the pre-baseline. For Granger causality connectivity, there is evident modulation for most emotions in the delta and beta bands, consistent with other graph analyses, as well as for some emotions like fear, jealousy, and relief in the alpha band, relative to the pre-baseline.

Discussion

Our study reveals nuanced patterns of EEG connectivity associated with various emotional states and highlights the neural complexity underlying both positive and negative emotions. Coherence analysis

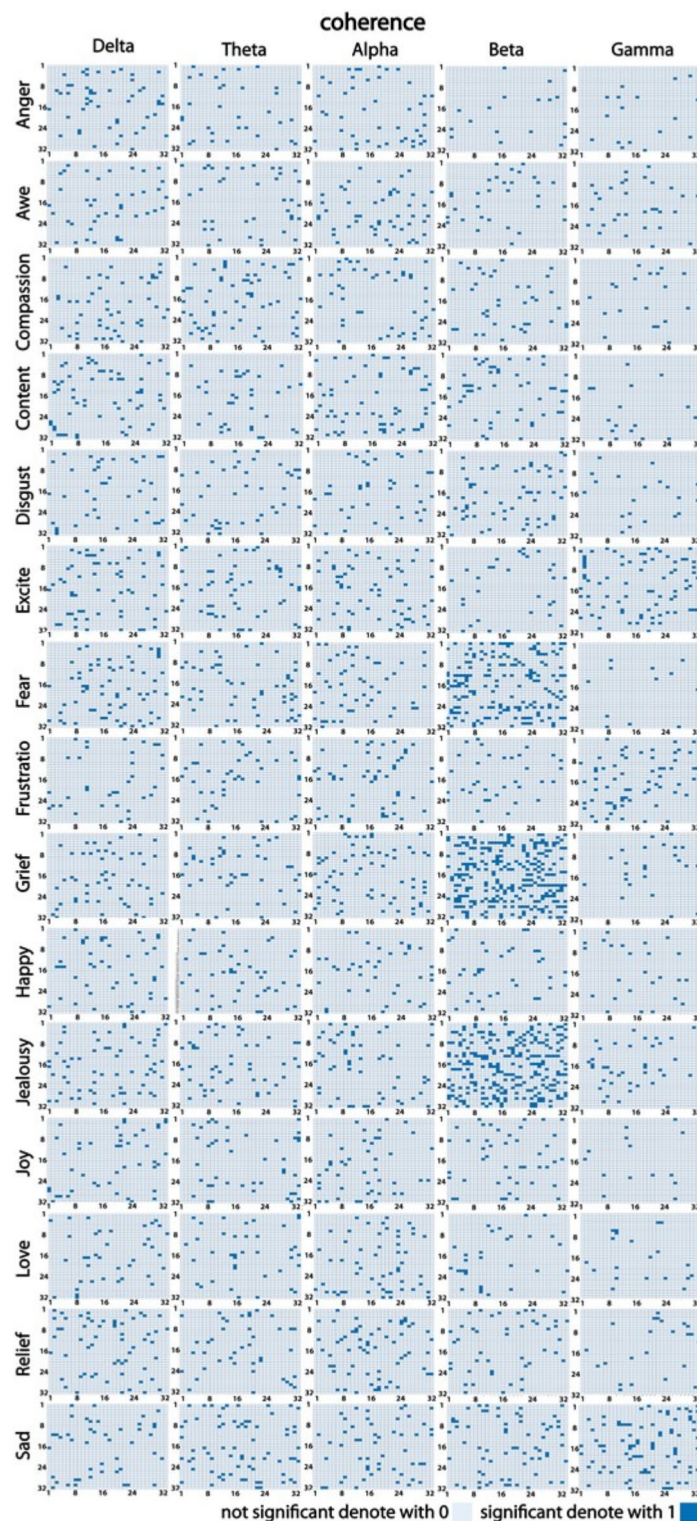


Fig. 3. Coherence connectivity measure. Statistical comparison of coherence connectivity measures across all frequency bands for each brain region, comparing eight positive and seven negative emotions to pre-baseline activity. Significant changes are indicated by 1, while non-significant changes are indicated by 0

identified predominant alpha-band activity across all emotional states, while significant beta-band activity was observed during negative emotions such as fear, grief, and jealousy, potentially reflecting heightened neural synchronization in these states. Additionally, gamma band activity increased significantly during emotions such as excitement, frustration, jealousy, and sadness. Granger causality analysis indicated a dominance of beta and

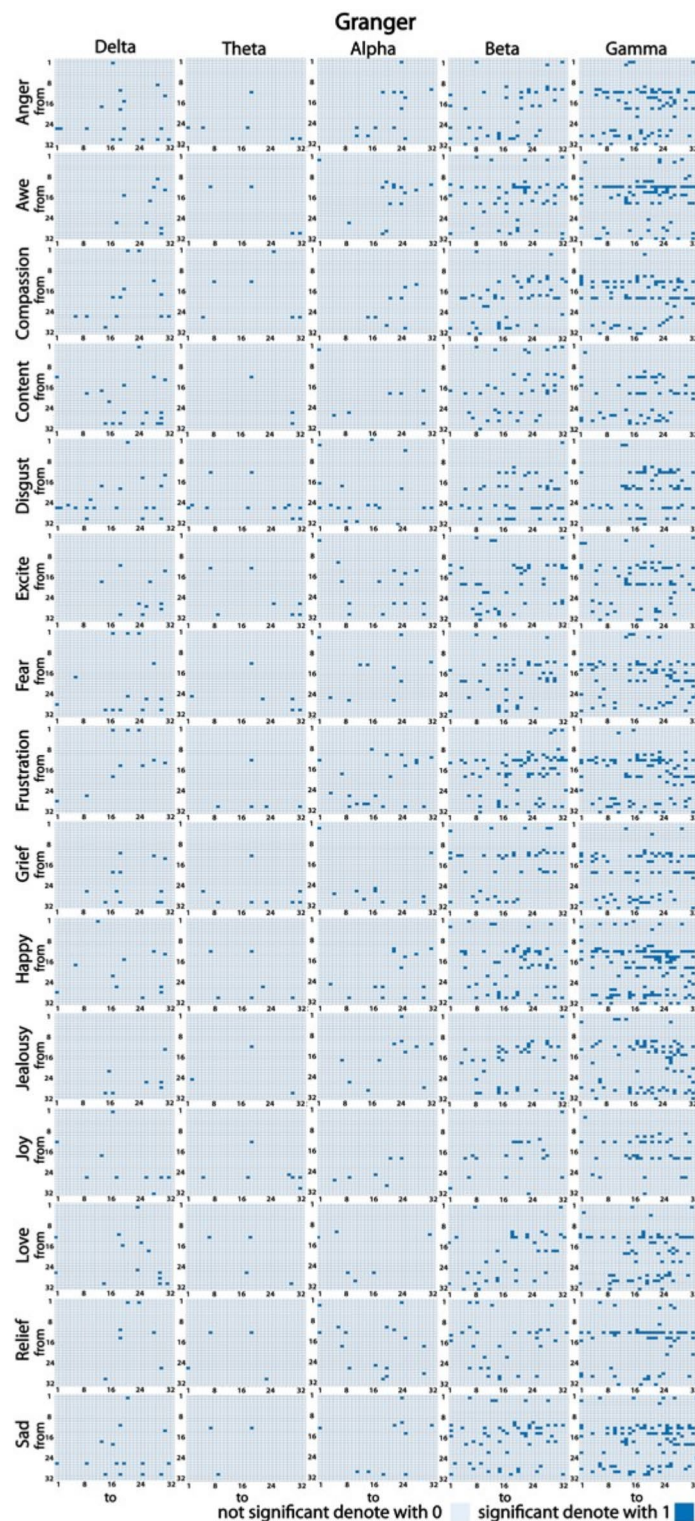


Fig. 4. Granger causality connectivity measure. Statistical comparison of Granger causality connectivity measures across all frequency bands for each brain region, comparing eight positive and seven negative emotions to pre-baseline activity. Significant changes are indicated by 1, while non-significant changes are indicated by 0. Rows of each matrix represent information “from” a brain region, while columns represent information “to” a brain region.

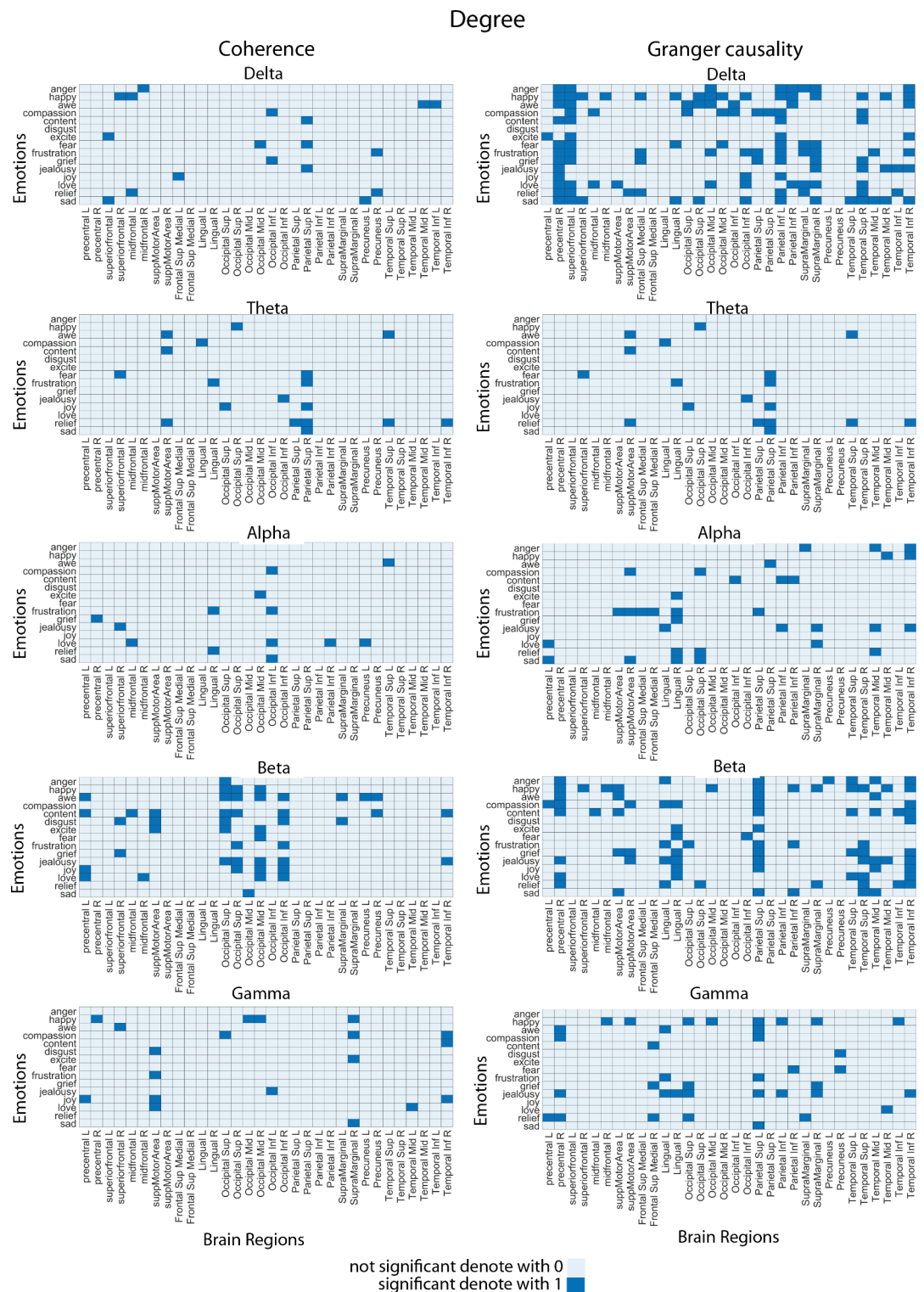


Fig. 5. Graph analysis measure. The figure illustrates a statistical comparison of the degree measure, indicating significant modulation (labeled 1) between specific emotions and pre-baseline activity in each brain region and the absence of substantial modulation (labeled 0). The first column presents the coherence connectivity results in different frequency bands, while the second column details the Granger causality connectivity results. Each subplot indicates whether each emotion shows modulation in each brain region based on degree measures for either coherence or Granger causality.

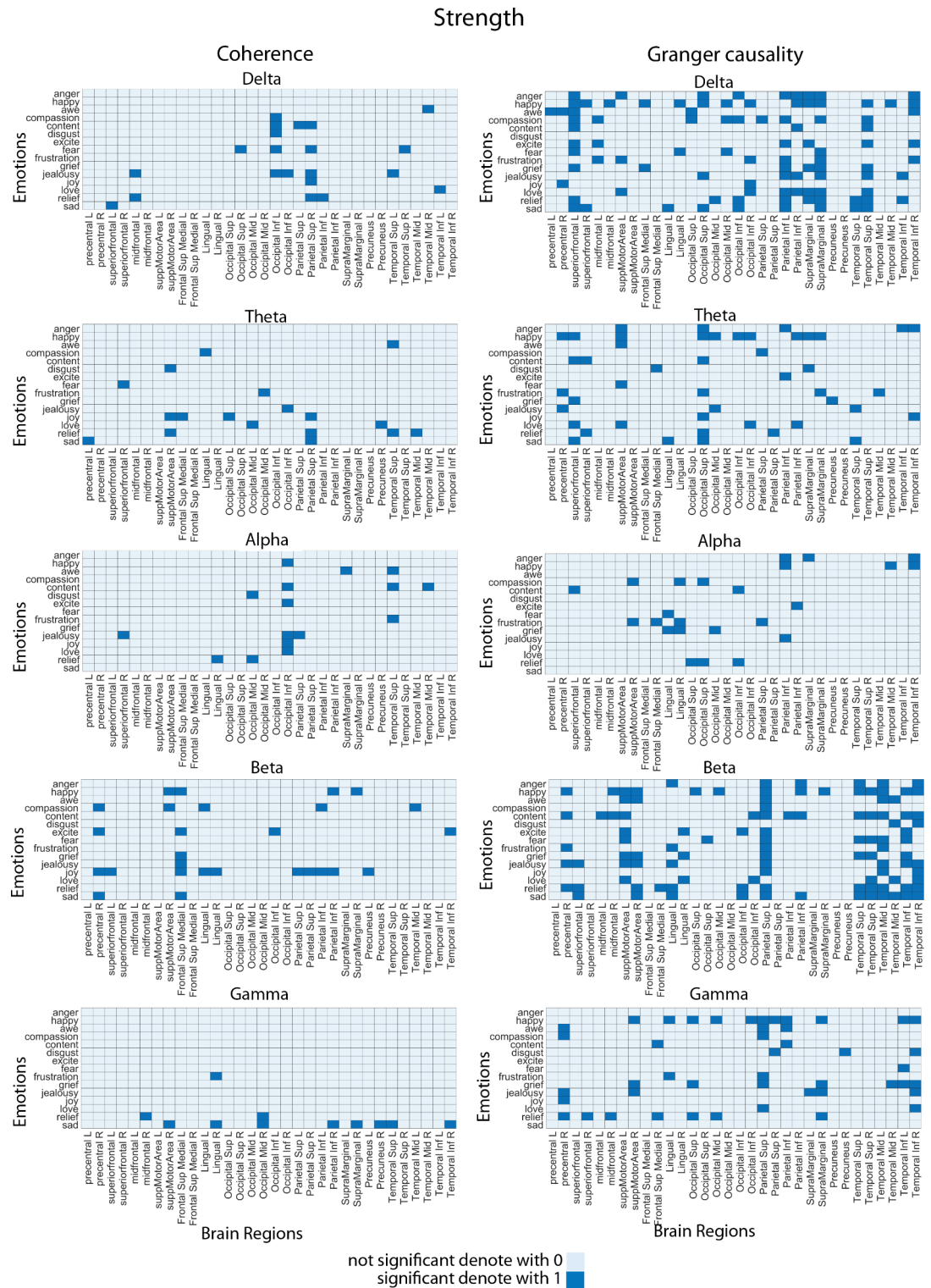


Fig. 6. Graph analysis measure. The figure illustrates a statistical comparison of the strength measure, indicating significant modulation (labeled 1) between specific emotions and pre-baseline activity in brain regions, and the absence of noteworthy modulation (labeled 0). The first column presents Coherence connectivity results in various frequency bands, while the second column details Granger causality connectivity outcomes. Each subplot indicates whether each emotion shows modulation in each brain region based on strength measures for either coherence or Granger causality.

Modularity

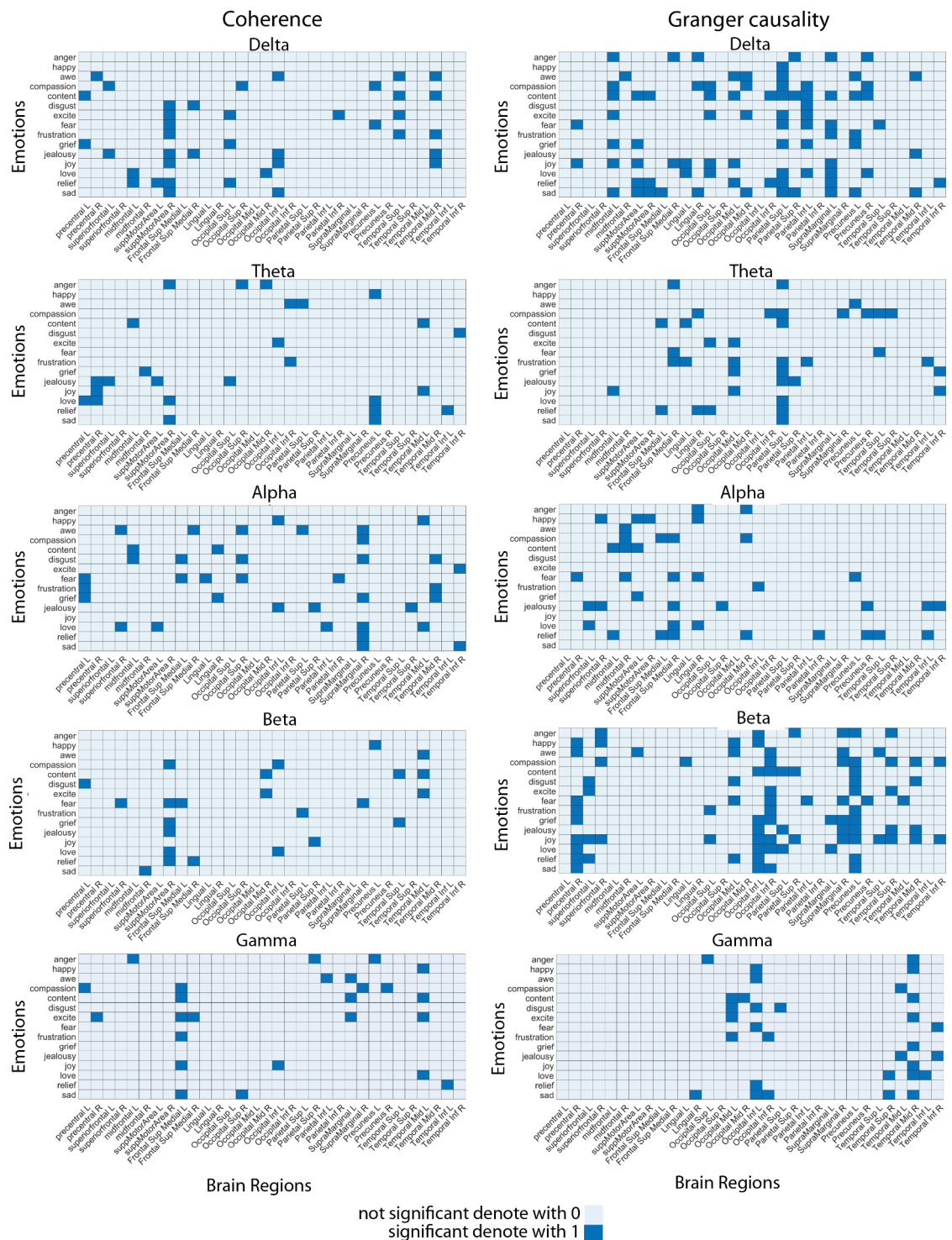


Fig. 7. Graph analysis measure. The figure illustrates a statistical comparison of the modularity measure, indicating significant modulation (labeled 1) between specific emotions and pre-baseline activity in brain regions, and the absence of substantial modulation (labeled 0). The first column presents Coherence connectivity results in various frequency bands, while the second column details Granger causality connectivity outcomes. Each subplot indicates whether each emotion shows modulation in each brain region based on modularity measures for either coherence or Granger causality.



Fig. 8. Comparative Graph Analysis of Emotional and Pre-baseline Activity. This figure represents a statistical comparison between various emotions and pre-baseline activity in different frequency bands. A value of 1 indicates significant differences between a given emotion and pre-baseline activity within a given frequency band, while a value of 0 indicates no significant difference. The first row shows results for coherence connectivity, and the second row displays results for Granger causality connectivity. The first column contains details about the cluster coefficients, the second column relates to density, and the last column contains the results of the transitivity measurement.

gamma bands across emotional states, with minimal modulation in the theta band, underscoring the critical role of higher frequency bands in emotional processing.

Regional analysis revealed that activity was primarily localized in the right lobe during episodes of sadness, involving areas such as the supplementary motor area, lingual gyrus, occipital midline, inferior parietal, supramarginal, and inferior temporal regions. Beta band activity was notably prominent in the temporal regions across nearly all emotional states. Importantly, coherence modularity highlighted activity in the lingual and superior medial frontal areas during negative emotions, while Granger causality modularity indicated intermittent gamma band activity, particularly in the occipital midline, inferior regions, and middle temporal areas. Figure 9 illustrates the connected brain regions (indicated by red circles) and the disconnected regions (indicated by gray circles) during emotional imagination, as visualized using the BrainNet Viewer MATLAB toolbox (<http://www.nitrc.org/projects/bnv/>)⁴⁵. Regions such as the frontal superior medial area, supplementary motor area, inferior parietal lobe, lingual gyrus, temporal regions, and inferior occipital areas exhibited connectivity, while others did not.

The lack of interactions in specific regions, despite their established roles in other cognitive or emotional tasks, indicates that these nodes may play a less central role in the emotional imagination paradigm employed in this study. For example, some frontal regions and parts of the cingulate cortex, which are frequently associated with emotion regulation, exhibited limited connectivity. This may reflect task-specific dynamics or methodological constraints, such as the sensitivity of coherence and Granger causality to particular types of interactions.

These findings offer valuable insights into the neural mechanisms underlying emotional processing. The predominance of alpha-band activity across all emotions may indicate a baseline level of cortical synchronization, while increased beta-band activity associated with negative emotions could reflect heightened arousal. Gamma band activity observed in emotions such as excitement and frustration highlights the significance of high-frequency oscillations in complex emotional experiences, likely indicating enhanced cognitive and emotional processing. The regional specificity, particularly the interactions within the right lobe network during sadness, aligns with previous research on emotional lateralization.

The modularity patterns observed in coherence and Granger causality provide evidence that emotional processing likely involves dynamic, region-specific neural networks. The disconnected regions identified in the study highlight potential pathways that may remain dormant during emotional imagination, offering additional avenues for exploration. These findings enhance our understanding of the neural basis of emotions and could inform targeted interventions in affective neuroscience, thereby aiding mental health treatments and advancing human-computer interaction technologies.

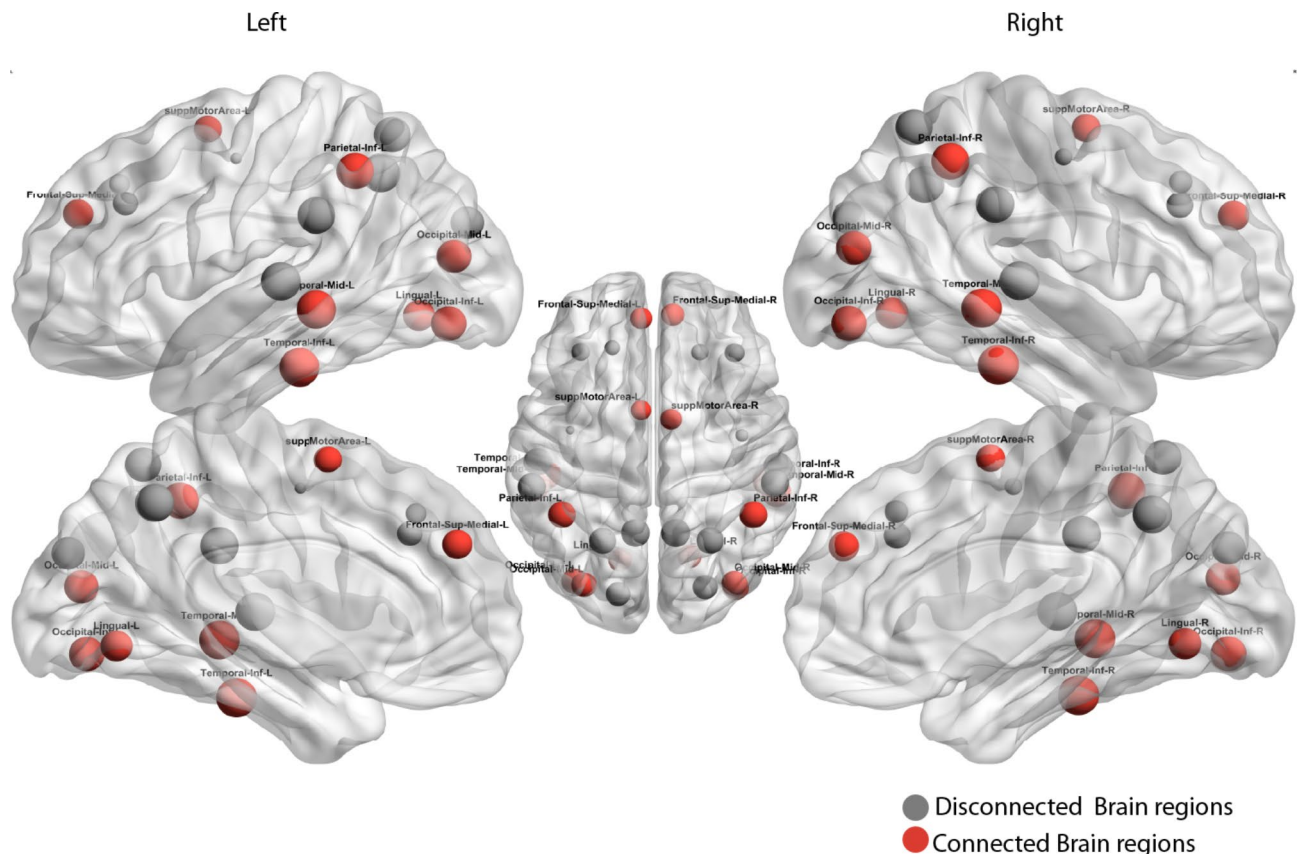


Fig. 9. Connected and disconnected brain regions during the emotion imagination task, generated using the BrainNet Viewer MATLAB toolbox. During the emotion imagination task, connected brain regions are highlighted with red circles, whereas disconnected areas are indicated with gray circles. The superior view is shown in the center, and the lateral view is shown on the side.

Our study builds upon the foundational research conducted by Onton and Makeig, particularly their investigation into high-frequency broadband modulation and the dynamics of emotional states as measured by EEG. They highlighted the significance of high-frequency broadband EEG modulations in cognitive and emotional tasks²⁹, a finding that aligns with our results, which demonstrate increased gamma band activity associated with emotions such as excitement, frustration, jealousy, and sadness. This aligns with their observations on the critical role of gamma oscillations in complex emotional and cognitive processes. Further researches highlighted the dynamic nature of emotional states and the potential of high-density EEG for unsupervised learning of these states^{34,35}, which complements our approach using coherence and Granger causality to elucidate frequency-specific connectivity patterns. Our results show regional specificity, such as right lobe gamma activity during sadness, aligning with the spatial dynamics reported in these studies. The application of ICA in our work to isolate cortical sources reflects the methodology advocated by Onton and Makeig and ensures robust data analysis. The Insights from Makeig and Onton Imagined Emotion Study³⁶ and their information-based modeling³¹ further contextualize our results within a broader framework of brain dynamics and emotional processing and highlight the utility of EEG in capturing the nuanced interplay of neural networks during emotional experiences. Our research serves to authenticate the findings of previous studies while presenting a comparative assessment of the neural correlates associated with positive and negative emotional experiences, thus facilitating a more holistic comprehension of the underlying mechanisms governing a diverse array of emotional states. Our findings contribute to the growing body of literature on the neural mechanisms underlying emotional processing and show several consistencies and novel insights compared to previous research. Notably, the predominant alpha band activity in all emotions in our coherence analysis aligns with the findings that alpha oscillations play a crucial role in regulating emotional states, particularly in maintaining a baseline level of cortical synchronization¹⁹. The significant beta band activity observed in negative emotions such as fear, grief, and jealousy is consistent with previous findings that beta band activity is associated with increased arousal and emotional intensity, particularly in response to negative stimuli⁵¹.

Increased gamma band activity during emotions such as excitement, frustration, jealousy, and sadness supports previous findings that illustrated the significance of gamma oscillations in merging sensory and cognitive functions during emotional episodes⁵². Furthermore, the regional specificity of gamma band activity in the right lobe during sadness, involving areas such as the supplementary motor area and the lingual gyrus, is

consistent with the results of a study that highlighted the role of the right hemisphere, specifically the prefrontal cortex during the processing of negative emotions⁵³.

Our Granger causality analysis revealing the dominance of beta and gamma bands in all emotions is in line with research that proposed the crucial role of these higher frequency bands in facilitating the effective communication of emotional data across various brain regions⁵⁴. The minimal modulation observed in the theta band contrasts with the findings that reported significant theta activity during emotional arousal, indicating potential differences in methodology or sample characteristics⁵⁵. Furthermore, the increased coherence connectivity in the gamma band during sadness and frustration may be consistent with the findings of Müller et al.⁵⁶, who showed that gamma coherence is related to the binding of emotional and cognitive processes, particularly in complex emotional states. The observed activity in regions such as the supplementary motor area and lingual gyrus during negative emotions aligns with studies by Etkin et al.⁵⁰, which emphasized the involvement of these areas in emotional regulation and sensory processing.

The collective analysis presented in our study supports numerous significant discoveries from prior research while offering novel perspectives on the frequency-specific and region-specific neural mechanisms involved in emotional processing. These contrasts emphasize the intricate nature of emotional encounters and highlight the significance of examining various frequency bands and brain regions to comprehend the neural foundation of emotions.

The results of our study have significant implications for both affective neuroscience and practical applications in mental health and human-computer interaction. Through the clarification of the unique neural dynamics linked to different emotional states, our research contributes to a deeper comprehension of the processing of diverse emotions within the brain. This knowledge is crucial for developing more effective and targeted mental health interventions. For instance, the observed signatures can inform the design of affective computing systems that more accurately recognize and respond to human emotions, improving user experience and interaction with technology. The regional specificity of emotional processing also provides insights into the neural circuits involved, which can guide future research in pinpointing the exact mechanisms underlying emotional regulation and dysregulation. Overall, our findings contribute to a deeper understanding of emotional processing, paving the way for innovative approaches to treating emotional disorders and enhancing human-computer interaction.

Despite its contributions, our study has several limitations. The sample size was relatively small, which may limit the generalizability of the results. Using a single dataset limits the diversity of emotional stimuli and contexts. Furthermore, while coherence, Granger causality, and graph theory analysis provide valuable insights, they have inherent methodological limitations, such as sensitivity to noise and assumptions about the linearity of neural interactions. Future studies should aim to overcome these constraints by utilizing broader and more varied samples, as well as employing multimodal methodologies to comprehensively examine the intricacies of emotional processing.

Future research should focus on expanding the scope of emotional states studied, including more nuanced and complex emotions. Longitudinal studies could provide insights into the stability and variability of connectivity patterns over time. Integrating other neuroimaging techniques, such as fMRI and MEG, could offer complementary perspectives on the temporal and spatial dynamics of emotional processing. Additionally, exploring the influence of individual differences, such as personality traits and genetic factors, could enhance our understanding of the neural underpinnings of emotional experiences. These pathways will provide additional clarity on the complex relationship between brain connectivity and emotional states and contribute to the advancement of both theoretical understanding and practical implementation.

Conclusion

In summary, this study provides an inclusive analysis of EEG connectivity patterns in different emotional states and reveals different frequency-specific and region-specific neural dynamics. Our results highlight the predominance of alpha band activity in all emotions, the significant role of beta band activity in negative emotions, and the enhanced gamma band activity in complex emotional states such as excitement, frustration, jealousy, and sadness. The Granger causality results underscored the dominance of beta and gamma bands in emotional processing, with minimal modulation in the theta band. The regional analysis also identified specific brain areas involved in different emotions, such as network interaction of the right lobe of the brain during sadness. These discoveries contribute to our understanding of the brain mechanisms that underlie emotional processing and have significant ramifications for the development of focused interventions in mental health and the advancement of affective computing systems. Our study highlights the importance of considering multiple frequency bands and brain regions in future research on emotional processing and lays the foundation for innovative approaches in neuroscience and technology.

Data availability

You can access the data directly on the NEMAR website (https://nemar.org/dataexplorer/detail?dataset_id=ds003004; look for Imagined Emotion Study).

Received: 25 September 2024; Accepted: 7 January 2025

Published online: 16 January 2025

References

1. Lerner, J. S., Li, Y., Valdesolo, P. & Kassam, K. S. Emotion and decision making. *Annu. Rev. Psychol.* **66**, 799–823. <https://doi.org/10.1146/annurev-psych-010213-115043> (2015).
2. Zhao, Y., Wang, D., Wang, X. & Chiu, S. C. Brain mechanisms underlying the influence of emotions on spatial decision-making: An EEG study. *Front. Neurosci.* **16**, 1–16. <https://doi.org/10.3389/fnins.2022.989988> (2022).

3. Aday, J., Rizer, W. & Carlson, J. M. Neural mechanisms of emotions and affect. in *Emotions and Affect in Human Factors and Human-Computer Interaction* 27–87, (Elsevier Academic, 2017). <https://doi.org/10.1016/B978-0-12-801851-4.00002-1>.
4. Celeghin, A., Diano, M., Bagnis, A., Viola, M. & Tamietto, M. Basic emotions in human neuroscience: Neuroimaging and beyond. *Front. Psychol.* **8**, 1–13. <https://doi.org/10.3389/fpsyg.2017.01432> (2017).
5. Panksepp, J. *Affective Neuroscience: The Foundations of Human and Animal Emotions* at Oxford University Press. <https://doi.org/10.1093/oso/9780195096736.001.0001> (1998).
6. Si, X., Huang, D., Sun, Y. & Ming, D. Temporal aware mixed attention-based convolution and transformer network (MACTN) for EEG emotion recognition. *arXiv:2305.18234* (2023).
7. Zhang, Z., Fort, J. M. & Giménez Mateu, L. Mini review: Challenges in EEG emotion recognition. *Front. Psychol.* **14**, 1–8. <https://doi.org/10.3389/fpsyg.2023.1289816> (2024).
8. Liu, R. et al. ERTNet: an interpretable transformer-based framework for EEG emotion recognition. *Front. Neurosci.* **18**, 1–11. <https://doi.org/10.3389/fnins.2024.1320645> (2024).
9. Gross, J. J. Emotion regulation: Current status and future prospects. *Psychol. Inq.* **26**, 1–26 (2015).
10. McRae, K. & Gross, J. J. Emotion regulation. *Emotion* **20**, 1–9. <https://doi.org/10.1037/emo0000703> (2020).
11. Lee, Y. Y. & Hsieh, S. Classifying different emotional states by means of EEG-based functional connectivity patterns. *PLoS One* **9**, e95415. <https://doi.org/10.1371/journal.pone.0095415> (2014).
12. Abhang, P. A., Gawali, B. W. & Mehrotra, S. C. *Introduction to EEG-and Speech-Based Emotion Recognition* (Academic, 2016).
13. Liu, C., Wang, Y., Sun, X., Wang, Y. & Fang, F. Decoding six basic emotions from brain functional connectivity patterns. *Sci. China Life Sci.* **66**, 835–847. <https://doi.org/10.1007/s11427-022-2206-3> (2023).
14. Becker, H. et al. Emotion Recognition based on high-resolution EEG recordings and reconstructed brain sources. *IEEE Trans. Affect. Comput.* **11**, 244–257. <https://doi.org/10.1109/TAFFC.2017.2768030> (2020).
15. Cohen, M. X., Elger, C. E. & Ranganath, C. Reward expectation modulates feedback-related negativity and EEG spectra. *Neuroimage* **35**, 968–978. <https://doi.org/10.1016/j.neuroimage.2006.11.056> (2007).
16. Miskovic, V. et al. Frontal brain oscillations and social anxiety: a cross-frequency spectral analysis during baseline and speech anticipation. *Elsevier Sci.* <https://doi.org/10.1016/j.biopsycho.2009.11.010> (2010).
17. Babiloni, C. et al. Hippocampal, amygdala, and neocortical synchronization of theta rhythms is related to an immediate recall during rey auditory verbal learning test. *Hum. Brain Mapp.* **30**, 2077–2089. <https://doi.org/10.1002/hbm.20648> (2009).
18. Balconi, M. & Mazza, G. Lateralisation effect in comprehension of emotional facial expression: A comparison between EEG alpha band power and behavioural inhibition (BIS) and activation (BAS) systems. *Laterality* **15**, 361–384. <https://doi.org/10.1080/13576500902886056> (2010).
19. Knyazev, G. G. Motivation, emotion, and their inhibitory control mirrored in brain oscillations. *Neurosci. Biobehav. Rev.* **31**, 377–395. <https://doi.org/10.1016/j.neubiorev.2006.10.004> (2007).
20. Seth, A. K., Chorley, P. & Barnett, L. C. Granger causality analysis of fMRI BOLD signals is invariant to hemodynamic convolution but not downsampling. *Neuroimage* **65**, 540–555. <https://doi.org/10.1016/j.neuroimage.2012.09.049> (2013).
21. Rojas-Libano, D., Wimmer, R. D. & Kinsner, W. Directional interactions between brain regions during emotional memory recall: A Granger causality analysis. *Neuroimage* **85**, 212–224 (2014).
21. Schubring, D. & Schupp, H. T. Affective picture processing: alpha-and lower beta-band desynchronization reflects emotional arousal. *Psychophysiology* **56**, e13386 (2019).
23. Deshpande, G., Hu, X., Lacey, S. & Stilla, R. Effective connectivity during emotion perception: A Granger causality analysis of functional magnetic resonance imaging data. *Hum. Brain Mapp.* **32**, 1280–1292 (2011).
24. Aydın, S. & Onbaşı, L. Graph theoretical brain connectivity measures to investigate neural correlates of music rhythms associated with fear and anger. *Cogn. Neurodyn.* **18**, 49–66. <https://doi.org/10.1007/s11571-023-09931-5> (2024).
25. Kılıç, B. & Aydın, S. Classification of contrasting discrete emotional states indicated by EEG based graph theoretical network measures. *Neuroinformatics* **20**, 863–877. <https://doi.org/10.1007/s12021-022-09579-2> (2022).
26. Cohen, M. X. *Analyzing Neural Time Series Data: Theory and Practice* (MIT Press, 2014).
27. Bassett, D. S. & Bullmore, E. Small-world brain networks. *Neurosci. Rev. J. Bringing Neurobiol. Neurol. Psychiatry* **12**, 512–523. <https://doi.org/10.1177/1073858406293182> (2006).
28. Bullmore, E. & Sporns, O. Complex brain networks: Graph theoretical analysis of structural and functional systems. *Nat. Rev. Neurosci.* **10**, 186–198. <https://doi.org/10.1038/nrn2575> (2009).
29. Palaniyappan, L. & Liddle, P. F. Diagnostic discontinuity in psychosis: A combined study of cortical gyrification and functional connectivity. *Schizophr. Bull.* **40**, 675–684 (2014).
30. Miskovic, V. & Schmidt, L. A. Cross-regional cortical synchronization during affective image viewing. *Brain Res.* **1362**, 102–111 (2010).
31. Onton, J. & Makeig, S. Information-based modeling of event-related brain dynamics. *Prog. Brain Res.* **159**, 99–120. [https://doi.org/10.1016/S0079-6123\(06\)59007-7](https://doi.org/10.1016/S0079-6123(06)59007-7) (2006).
32. Onton, J. & Makeig, S. High-frequency broadband modulation of electroencephalographic spectra. *Front. Hum. Neurosci.* **3**, 1–18. <https://doi.org/10.3389/fpsyg.2009.061.2009> (2009).
33. Banks, S. J., Eddy, K. T., Angstadt, M., Nathan, P. J. & Phan, K. L. Amygdala-frontal connectivity during emotion regulation. *Soc. Cogn. Affect. Neurosci.* **2**, 303–312. <https://doi.org/10.1093/scan/nsm029> (2007).
34. Hsu, S. H., Lin, Y., Onton, J., Jung, T. P. & Makeig, S. Unsupervised learning of brain state dynamics during emotion imagination using high-density EEG. *Neuroimage* **249**, 118873. <https://doi.org/10.1016/j.neuroimage.2022.118873> (2022).
35. Kothe, C. A., Makeig, S. & Onton, J. A. Emotion recognition from EEG during self-paced emotional imagery. in *2013 Humaine Association Conference on Affective Computing and Intelligent Interaction* 855–858. <https://doi.org/10.1109/ACII.2013.160> (2013).
36. Makeig, S. & Onton, J. Imagined emotion study. *OpenNeuro*. <https://doi.org/10.18112/openneuro.ds003004.v1.1.1> (2022).
37. Delorme, A. & Makeig, S. EEGLAB: an open source toolbox for analysis of single-trial EEG dynamics including independent component analysis. *J. Neurosci. Methods* **134**, 9–21. <https://doi.org/10.1016/j.jneumeth.2003.10.009> (2004).
38. Delorme, A., Sejnowski, T. & Makeig, S. Enhanced detection of artifacts in EEG data using higher-order statistics and independent component analysis. *Neuroimage* **34**, 1443–1449. <https://doi.org/10.1016/j.neuroimage.2006.11.004> (2007).
39. Rho, G., Callara, A. L., Bernardi, G., Scilingo, E. P. & Greco, A. EEG cortical activity and connectivity correlates of early sympathetic response during cold pressor test. *Sci. Rep.* **13**, 1338. <https://doi.org/10.1038/s41598-023-27480-z> (2023).
40. Makeig, S., Jung, T. P., Bell, A. J., Ghahremani, D. & Sejnowski, T. J. Blind separation of auditory event-related brain responses into independent components. *Proc. Natl. Acad. Sci. U. S. A.* **94**, 10979–10984. <https://doi.org/10.1073/pnas.94.20.10979> (1997).
41. Pion-Tonachini, L., Kreutz-Delgado, K. & Makeig, S. ICLabel: an automated electroencephalographic independent component classifier, dataset, and website. *Neuroimage* **198**, 181–197. <https://doi.org/10.1016/j.neuroimage.2019.05.026> (2019).
42. Oostenveld, R., Fries, P., Maris, E. & Schoffelen, J. M. FieldTrip: Open source software for advanced analysis of MEG, EEG, and invasive electrophysiological data. *Comput. Intell. Neurosci.* **2011**, 156869. <https://doi.org/10.1155/2011/156869> (2011).
43. Yu, B. et al. Aberrant whole-brain functional connectivity and intelligence structure in children with primary nocturnal enuresis. *PLoS One* **8**, e51924. <https://doi.org/10.1371/journal.pone.0051924> (2013).
44. Tzourio-Mazoyer, N. et al. Automated anatomical labeling of activations in SPM using a macroscopic anatomical parcellation of the MNI MRI single-subject brain. *Neuroimage* **15**, 273–289 (2002).
45. Xia, M., Wang, J. & He, Y. BrainNet Viewer: a network visualization tool for human brain connectomics. *PLoS One* **8**, e68910. <https://doi.org/10.1371/journal.pone.0068910> (2013).

46. Andrzejak, R. G. et al. Indications of nonlinear deterministic and finite-dimensional structures in time series of brain electrical activity: Dependence on recording region and brain state. *Phys. Rev. E*. **64**, 61907. <https://doi.org/10.1103/PhysRevE.64.061907> (2001).
47. Rubinov, M. & Sporns, O. Complex network measures of brain connectivity: Uses and interpretations. *Neuroimage* **52**, 1059–1069. <https://doi.org/10.1016/j.neuroimage.2009.10.003> (2010).
48. Fornito, A., Zalesky, A. & Bullmore, E. *Fundamentals of Brain Network Analysis* (Academic, 2016).
49. Farahani, F. V., Karwowski, W. & Lighthall, N. R. Application of graph theory for identifying connectivity patterns in human brain networks: A systematic review. *Front. Neurosci.* **13**, 585 (2019).
50. Olejarczyk, E. & Jernajczyk, W. Graph-based analysis of brain connectivity in schizophrenia. *PLoS One* **12**, e0188629. <https://doi.org/10.1371/journal.pone.0188629> (2017).
51. Balconi, M. & Lucchiari, C. EEG correlates (event-related desynchronization) of emotional face elaboration: A temporal analysis. *Neurosci. Lett.* **392**, 118–123. <https://doi.org/10.1016/j.neulet.2005.09.004> (2006).
52. Keil, A., Müller, M. M., Ray, W. J., Gruber, T. & Elbert, T. Human gamma band activity and perception of a gestalt. *J. Neurosci. Off J. Soc. Neurosci.* **19**, 7152–7161. <https://doi.org/10.1523/JNEUROSCI.19-16-07152.1999> (1999).
53. Davidson, R. J. What does the prefrontal cortex do in affect: Perspectives on frontal EEG asymmetry research. *Biol. Psychol.* **67**, 219–233. <https://doi.org/10.1016/j.biopsycho.2004.03.008> (2004).
54. Bressler, S. L. & Menon, V. Large-scale brain networks in cognition: Emerging methods and principles. *Trends Cogn. Sci.* **14**, 277–290. <https://doi.org/10.1016/j.tics.2010.04.004> (2010).
55. Aftanas, L. I., Varlamov, A. A., Pavlov, S. V., Makhnev, V. P. & Reva, N. V. Affective picture processing: Event-related synchronization within individually defined human theta band is modulated by valence dimension. *Neurosci. Lett.* **303**, 115–118. [https://doi.org/10.1016/S0304-3940\(01\)01703-7](https://doi.org/10.1016/S0304-3940(01)01703-7) (2001).
56. Müller, M. M., Keil, A., Gruber, T. & Elbert, T. Processing of affective pictures modulates right-hemispheric gamma band EEG activity. *Clin. Neurophysiol. Off J. Int. Fed. Clin. Neurophysiol.* **110**, 1913–1920. [https://doi.org/10.1016/S1388-2457\(99\)00151-0](https://doi.org/10.1016/S1388-2457(99)00151-0) (1999).

Acknowledgements

We want to express our deep gratitude to the Neuroscience Research Center at Baqiyatallah University of Medical Sciences for their valuable support and resources that contributed significantly to the success of this study. We are also very grateful to Prof. Scott Makeig's team behind the “Imagined Emotion Study” project (https://n.umar.org/dataexplorer/detail?dataset_id=ds003004) for providing access to their comprehensive dataset plays a crucial role in our analysis. The availability of these high-quality EEG recordings contributed significantly to facilitating our research.

Author contributions

JO and SM collected the data. MR and HN analyzed the data and wrote the primary draft of the manuscript. Figures 1 and 9 were generated using the BrainNet Viewer MATLAB toolbox by MR. AM and SM did the project idea, leadership, editing, and finalizing of the manuscript.

Funding

This research did not receive any specific grant from funding agencies in the public, commercial, or not-for-profit sectors.

Declarations

Competing interests

The authors declare no competing interests.

Additional information

Supplementary Information The online version contains supplementary material available at <https://doi.org/10.1038/s41598-025-86040-9>.

Correspondence and requests for materials should be addressed to A.M.

Reprints and permissions information is available at www.nature.com/reprints.

Publisher's note Springer Nature remains neutral with regard to jurisdictional claims in published maps and institutional affiliations.

Open Access This article is licensed under a Creative Commons Attribution-NonCommercial-NoDerivatives 4.0 International License, which permits any non-commercial use, sharing, distribution and reproduction in any medium or format, as long as you give appropriate credit to the original author(s) and the source, provide a link to the Creative Commons licence, and indicate if you modified the licensed material. You do not have permission under this licence to share adapted material derived from this article or parts of it. The images or other third party material in this article are included in the article's Creative Commons licence, unless indicated otherwise in a credit line to the material. If material is not included in the article's Creative Commons licence and your intended use is not permitted by statutory regulation or exceeds the permitted use, you will need to obtain permission directly from the copyright holder. To view a copy of this licence, visit <http://creativecommons.org/licenses/by-nc-nd/4.0/>.

© The Author(s) 2025